# Proton MR Spectroscopy of Delayed Cerebral Radiation in Monkeys and Humans after Brachytherapy

Kimihisa Kinoshita, Eiji Tada, Kengo Matsumoto, Shoji Asari, Takashi Ohmoto, and Takahiko Itoh

**PURPOSE:** To determine whether radiation necrosis can be differentiated from residual/recurrent tumor by proton MR spectroscopy. **METHODS:** We studied the effects of interstitial brachytherapy on the brains of healthy monkeys and in humans with glioblastoma multiforme. The effects of radiation therapy on normal brain tissue in monkeys were assessed with sequential proton MR spectroscopic studies 1 week to 6 months after brachytherapy. Proton MR spectroscopy was also performed in five patients with residual/recurrent glioblastoma multiforme (three of whom had radiation necrosis after brachytherapy), seven patients with newly diagnosed untreated glioblastoma multiforme, and 16 healthy volunteers, who served as a control group. **RESULTS:** In monkeys, the ratio of *N*-acetylaspartate (NAA) to creatine-phosphocreatine (Cr) and the ratio of choline-containing compounds (Cho) to Cr of the reference point were significantly lower 1 week after brachytherapy than before treatment. The ratio of NAA to Cho of the irradiated area tended to be higher 1 week after brachytherapy than before irradiation. These peak metabolic ratios showed characteristic changes 6 months after treatment. In two of three monkeys, lipid signal was elevated 6 months after irradiation. In the clinical study, the ratio of NAA to Cho in the area of radiation necrosis was significantly different from that in glioblastoma multiforme when compared with the contralateral hemisphere after irradiation. In addition, lipid signal was detected in all patients with radiation necrosis. **CONCLUSION:** It might be possible to use proton MR spectroscopy to differentiate radiation necrosis from residual/recurrent glioblastoma multiforme on the basis of comparisons with the contralateral hemisphere after radiation therapy.

**Index terms:** Animal studies; Glioblastoma multiforme; Radiation, necrosis

*AJNR Am J Neuroradiol* 18:1753–1761, October 1997

The efficacy of interstitial irradiation in the treatment of malignant brain tumors is well established (1–3). Radiation necrosis commonly occurs after brachytherapy, but it is difficult to differentiate from tumor recurrence with computed tomography (CT) or magnetic resonance (MR) imaging.

MR spectroscopy is a noninvasive method used to determine intracellular pathophysiological conditions (4–8). A few investigators have described the changes seen at MR spectroscopy after external radiation therapy (9, 10). We analyzed the features of proton MR spectroscopy in monkey brains damaged by brachytherapy and in patients with glioblastoma multiforme treated with interstitial brachytherapy in an attempt to differentiate radiation necrosis from residual/recurrent brain tumor.

## Materials and Methods

### *Experimental Studies*

Six adult Japanese monkeys (*Macaca fuscata*) weighing 4.2 to 6.1 kg (mean, 5.2 kg) were used in this study. All animals were housed individually under standard conditions and given routine care by trained animal technicians. During the period of irradiation, the monkeys were housed in radioprotected area. This experiment was carried out according to the Animal Experiment Guide of our institution. The animals were observed daily for the entire course of the study, and notes were made of each monkey's motor and behavioral characteristics, including responses to an examiner and reactions to hand-fed bits of fruit. The effects of radiation on normal brain tissue were assessed

Received December 16, 1996; accepted after revision April 1, 1997.

From the Department of Neurological Surgery, Okayama University Medical School, 2–5–1 Shikata-cho, Okayama, Japan. Address reprint requests to Kimihisa Kinoshita, MD.

AJNR 18:1753–1761, Oct 1997 0195-6108/97/1809–1753

with sequential MR imaging and proton MR spectroscopy 1 week and 1 month after brachytherapy in all six monkeys. Further studies were done 3 months after treatment in five monkeys and 6 months after treatment in three monkeys.

For anesthesia, each monkey was given ketamine hydrochloride (10 mg/kg) and atropine sulfate (0.06 mg/kg) intramuscularly, and an intravenous catheter was introduced into a calf vein. Lactate Ringer's solution was infused through this catheter. All animals were maintained with pentobarbital (15 mg/kg), which was administered as an intravenous bolus and supplemented with 5 mg/kg as needed throughout the various procedures.

### *Brachytherapy*

A right frontal craniotomy was done, and an iridium-192 seed assembly was inserted stereotactically into each monkey's brain 7 mm to the right of the midline, 22 mm deep, 22 mm anterior to the interaural line, and perpendicular to the plane passing through both external auditory meatus and the inferior orbital ridge (the H-O plane).

The reference point was defined by a plane passing through the midpoint of the seed assembly (11 mm deep to the brain surface) in the white matter 5 mm from the seed assembly. The seed assembly had an average activity of 12 mCi. The dose rate at the reference point averaged 112 cGy/h. A total dose of 202 Gy was applied at the reference point over a period of 181 hours. The volume of brain tissue receiving more than the total dose of 202 Gy was approximately 1.5 $cm^3$. Total doses were calculated with a computerized radiation treatment planner (Modulex, Computerized Medical System, St Louis, Mo).

### *MR Imaging*

MR imaging was done with a 1.5-T clinical system. T1-weighted images with and without 0.3 mmol/kg of gadopentetate dimeglumine were obtained using a spin-echo sequence of 500/13/3 (repetition time/echo time/excitations). T2-weighted images were obtained with a fast spin-echo sequence of 4000/95/2, with an echo train length of eight. All images were obtained with a 256 × 128 matrix, a 13-cm field of view, and section thickness of 3 mm with a 0.5-mm intersection gap. These parameters resulted in six oblique-axial images, which included the plane parallel to the H-O plane and passed through the reference point. These MR studies were obtained 1 week, 1 month, 3 months, and 6 months after irradiation.

### *Proton MR Spectroscopy*

Proton MR spectroscopy was performed with the same 1.5-T clinical system, equipped with a bird cage–type head coil. The magnetic field homogeneity was adjusted by shimming on the proton signal using an automated routine provided in the unit's research package. We used a point-resolved spectroscopy sequence with a chemical shift-selective pulse for water suppression, because this technique offers a gain of a factor of two in signal-to-noise ratio, less sensitivity to motion and diffusion, and no sensitivity to multiple-quantum effect as compared with other sequences, such as stimulated-echo acquisition mode or image-selected in vivo spectroscopy (11).

The coordinates for a single volume of interest of 1.0 $cm^3$ centering on the reference point were established on the axial T2-weighted image. The size of all volumes of interest was fixed at 1.0 $cm^3$ to prevent contamination by subcutaneous fat and cerebrospinal fluid in the lateral ventricle. On the section through the reference point, the monkey brains were about 7 cm in anteroposterior diameter and 5 cm in transverse diameter. We used the minimum volume of interest possible for our clinical MR system. Acquisition parameters were 2000/136, with 192 to 384 scanning repetitions. The spectral width was 2500 Hz, and the number of data sample points was 2048. The scan time for the collection of proton MR spectroscopic data ranged from 6.5 to 13 minutes. These studies were also obtained 1 week, 1 month, 3 months, and 6 months after brachytherapy, and spectral data were acquired before the MR imaging studies.

The spectra were processed on a Sparcstation (Sun Microsystems, Mountain View, Calif) with installed SA/GE spectroscopic analysis software (General Electric Medical Systems, Milwaukee, Wis). The resulting free induction decay was rectified with an exponential line-broadening of 2 Hz after zero-filling to 4096 points. After one-dimensional Fourier transformation, a phase correction was applied. The spectra were evaluated without baseline correction programs. The single-volume data were processed by applying the Lorentz-Gauss transformation for noise reduction. To determine the peak ratios of metabolites, the peak heights and areas of each metabolite were measured from baseline. The major metabolites for our interests included the $CH_3$ group of *N*-acetylaspartate (NAA) at 2.0 ppm, the $CH_3$ group of creatine-phosphocreatine (Cr) at 3.0 ppm, the $(CH_3)_3$ group of choline-containing compounds (Cho) at 3.2 ppm, and the $CH_3$ group of lactate at 1.3 ppm.

We analyzed these metabolites as ratios to peak intensities (NAA/Cr, Cho/Cr, and NAA/Cho). These peak ratios were compared with the ratios before irradiation and with the ratios of the corresponding contralateral white matter.

### *Clinical Studies*

MR imaging and proton MR spectroscopy were performed in five patients (43 to 62 years old; mean age, 50 years) with residual/recurrent glioblastoma multiforme treated by brachytherapy, including three patients (44 to 62 years old; mean age, 51 years) with proved radiation necrosis. Imaging studies were also performed in seven patients (32 to 68 years old; mean age, 55 years) with newly diagnosed glioblastoma multiforme and in 16 volunteers (20 to 39 years old; mean age, 25 years) who served as a control group. Three patients with radiation necrosis are still alive; the patient with the longest survival time is 4 years past the first operation. Six patients with

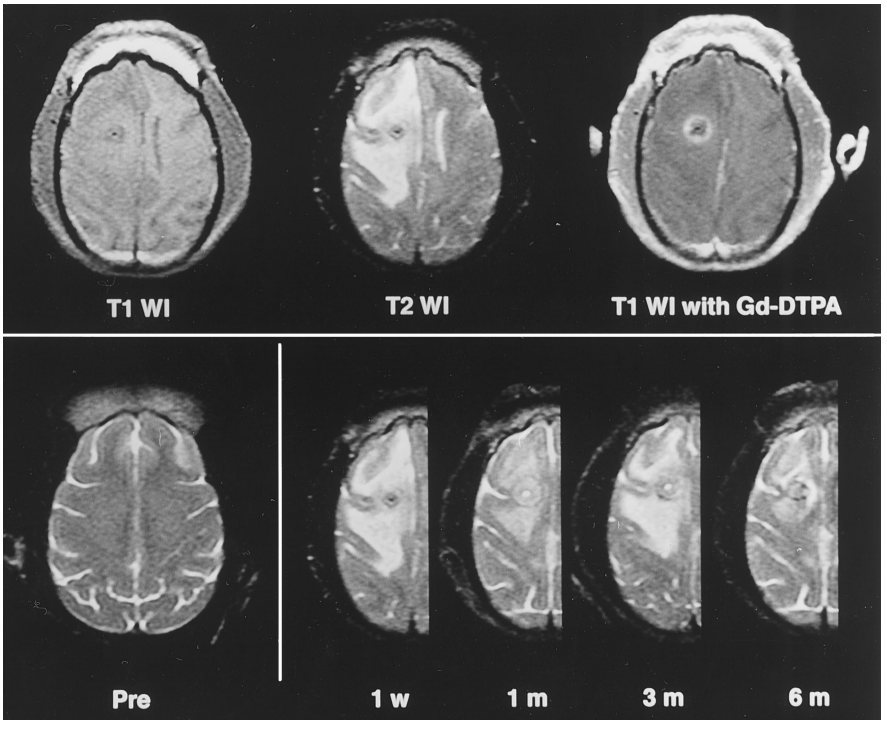


Fig 1. *Top row*, MR images of a monkey brain 1 week after brachytherapy. *Left*, T1-weighted image (500/13/3) shows a hypointense area around the placement tract of the seed assembly; *center*, T2-weighted image (4000/95/2) shows a large hyperintense area in white matter with midline shift; *right*, T1-weighted image with contrast enhancement shows ring enhancement around the tract.

*Bottom row*, Sequential T2-weighted MR images of a monkey brain treated with brachytherapy before irradiation (*left*) and 1 week, 1 month, 3 months, and 6 months after treatment, respectively (*right*). The hyperintense area and the mass effect were less prominent 1 month after irradiation and again at 6 months.

newly diagnosed or residual/recurrent glioblastoma multiforme are also alive, but three others have died.

MR imaging was performed with the same clinical system used for the monkey studies. T1-weighted images with and without 0.1 mmol/kg gadopentetate dimeglumine were obtained with a spin-echo sequence of 500/18/2. T2-weighted images were obtained with a fast spin-echo sequence of 4000/114/2 and an echo train length of eight. All images were obtained with a 256 × 192 matrix, a 22-cm field of view, and a 6-mm section thickness with a 2-mm intersection gap. These parameters resulted in 12 oblique axial images, which included a plane passing through the nasion and the pontomedullary junction on the midsagittal scout image.

Proton MR spectroscopy was performed in the same manner as for the monkeys, except that the single volume of interest ranged in size from 1 to 8 $cm^3$ and was contained in the brain tumors or in the areas of radiation necrosis, which were established on the axial T1- or T2-weighted images. These studies in the cases of radiation necrosis were performed 17 to 22 months after brachytherapy. Spectral analysis was done in the same way as in the experimental studies.

Proton MR spectroscopic data from corresponding white matter of the contralateral hemisphere were used as controls. These clinical data were analyzed as ratios to major peak intensities. These peak metabolic ratios were compared with those of the contralateral hemisphere in the patients with tumors and in the healthy volunteers.

## Results

### *Experimental Studies*

The MR images taken 1 week after brachytherapy in one monkey are shown in Figure 1. The T1-weighted image showed a hypointense area around the placement tract of the seed assembly. The T2-weighted image showed a large hyperintense area in the white matter with midline shift. The contrast-enhanced T1-weighted image showed ring enhancement around the tract. In sequential T2-weighted MR images of a monkey treated with brachytherapy, the hyperintense area and mass effect were reduced 1 month after irradiation, and nearly stable thereafter.

Figure 2 shows sequential proton MR spectra at the reference point before irradiation and at each point after brachytherapy. The NAA and Cho signals 1 week after irradiation were relatively lower than they were before treatment.

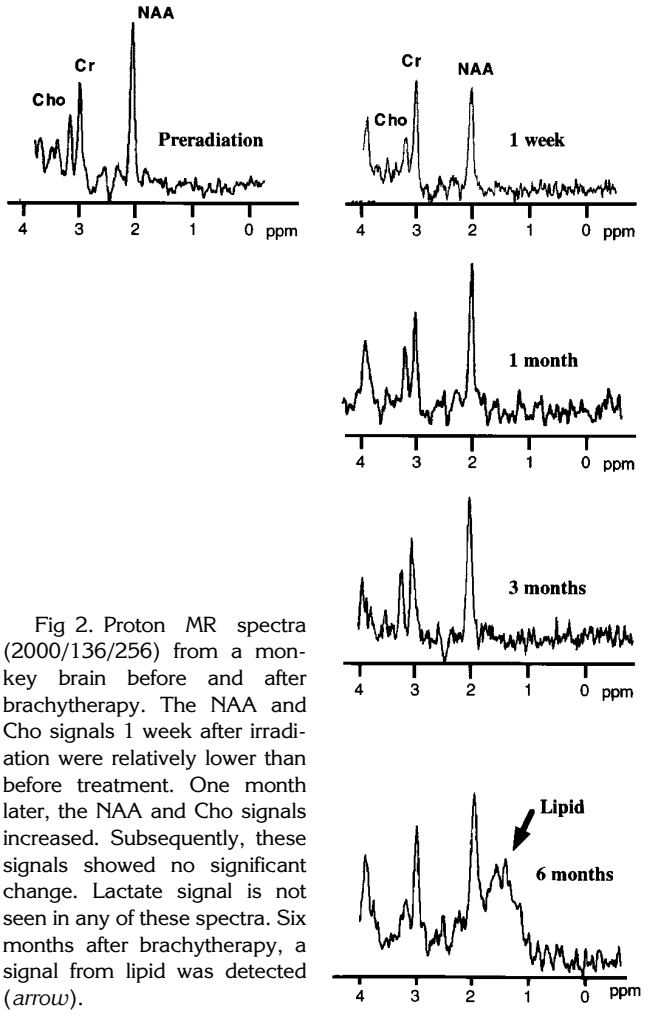


Fig 2. Proton MR spectra (2000/136/256) from a monkey brain before and after brachytherapy. The NAA and Cho signals 1 week after irradiation were relatively lower than before treatment. One month later, the NAA and Cho signals increased. Subsequently, these signals showed no significant change. Lactate signal is not seen in any of these spectra. Six months after brachytherapy, a signal from lipid was detected (*arrow*).

One month later, the NAA and Cho signals increased. Subsequently, these signals did not show rapid change. The lactate signal was not detected in any of the spectra. Spectra from two monkeys obtained 6 months after brachytherapy showed a signal from lipid.

Figure 3 is a graphic representation of the proton MR spectroscopic data. The ratios of NAA/Cr, Cho/Cr, and NAA/Cho before treatment were 1.830 ± 0.142, 0.759 ± 0.069, and 2.247 ± 0.118 (mean ± standard error), respectively. A statistical analysis of variance (ANOVA) of this data confirmed that the ratio of NAA/Cr (1.052 ± 0.072) and Cho/Cr (0.483 ± 0.090) decreased significantly 1 week after brachytherapy compared with the ratio before treatment (NAA/Cr, $P < .001$; Cho/Cr, $P = .033$). The NAA/Cr ratio at 6 months (1.119 ± 0.196) was lower than that before irradiation ($P = .061$). The Cho/Cr at 6 months (0.602 ± 0.040) was also lower than that before treatment ($P = .069$). Elevated peaks from lipid that had broad bases centering at approximately 1.2 ppm were observed at 6 months after irradiation in two of three monkeys. These signals might have been due to lipid-laden macrophages.

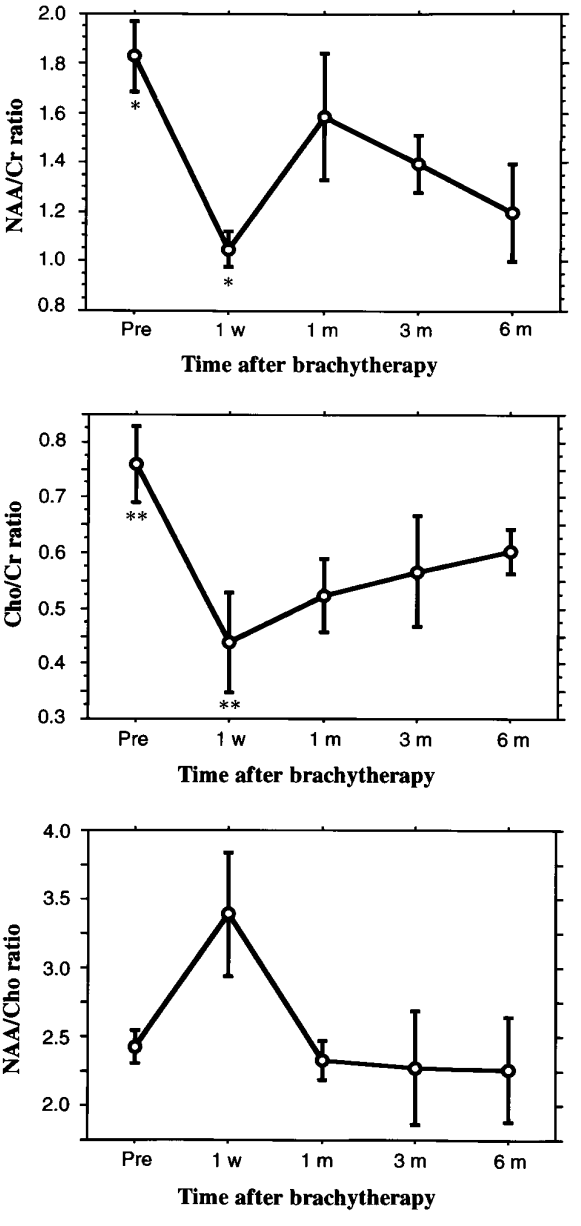


Fig 3. The time course of metabolic peaks at the reference point as shown by proton MR spectra of monkey brains irradiated by brachytherapy. The ratios of NAA/Cr and Cho/Cr decreased significantly 1 week after brachytherapy *Asterisk* indicates $P < .001$; *double asterisk*, $P = .033$.

The peak ratios between the reference point and the contralateral hemisphere 6 months after brachytherapy were nearly equal. The ratio between NAA/Cr at the reference point and in the contralateral hemisphere was 0.892 ± 0.071.

Similarly, the ratio of NAA/Cho was 0.908 ± 0.067, and the ratio of Cho/Cr was 0.983 ± 0.021. These results show that the ratios between each metabolic peak at the reference point and in the contralateral hemisphere after treatment approached 1.00. Analysis of proton MR spectroscopic data from the contralateral hemispheres, which received approximately 15 Gy, confirmed that brachytherapy had some effect on those (nonimplanted) hemispheres (Fig 4).

*Clinical Studies*

NAA/Cr, NAA/Cho, and Cho/Cr of tumors, including new diagnoses and recurrences, were 1.136 ± 0.170, 0.496 ± 0.071, and 2.403 ± 0.257, respectively. The NAA/Cr (1.136 ± 0.170) and the NAA/Cho (0.496 ± 0.071) in patients with glioblastoma multiforme were significantly lower than those in healthy volunteers (NAA/Cr, 2.150 ± 0.111; NAA/Cho, 2.089 ± 0.131, $P < .005$). The Cho/Cr in patients with glioblastoma multiforme was significantly higher than that in healthy volunteers (1.074 ± 0.078, $P < .005$) (Fig 5).

In three of 12 patients, radiation necrosis occurred after brachytherapy. In all three patients, it was not possible to differentiate radiation necrosis from residual/recurrent glioblastoma multiforme on MR images. Figure 6 shows typical spectra from a patient with glioblastoma multiforme and from a patient with radiation necrosis. Lipid signal was not observed in the patients with glioblastoma multiforme, but it did appear in the patients with radiation necrosis.

There were no significant differences between patients with radiation necrosis and those with glioblastoma multiforme with respect to NAA/Cr, NAA/Cho, and Cho/Cr. Thus, it was difficult to differentiate radiation necrosis from malignant gliomas on the basis of comparisons with the peak metabolic ratios in healthy control subjects.

Subsequently, we compared peak metabolic ratios from the lesions with those from the contralateral hemispheres after irradiation. The ratios of NAA/Cr, NAA/Cho, and Cho/Cr for glioblastoma multiforme as compared with corresponding ratios for the irradiated contralateral hemisphere were 0.542 ± 0.085, 0.242 ± 0.035, and 2.400 ± 0.241, respectively. The ratios of NAA/Cr, NAA/Cho, and Cho/Cr in patients with radiation necrosis as compared with

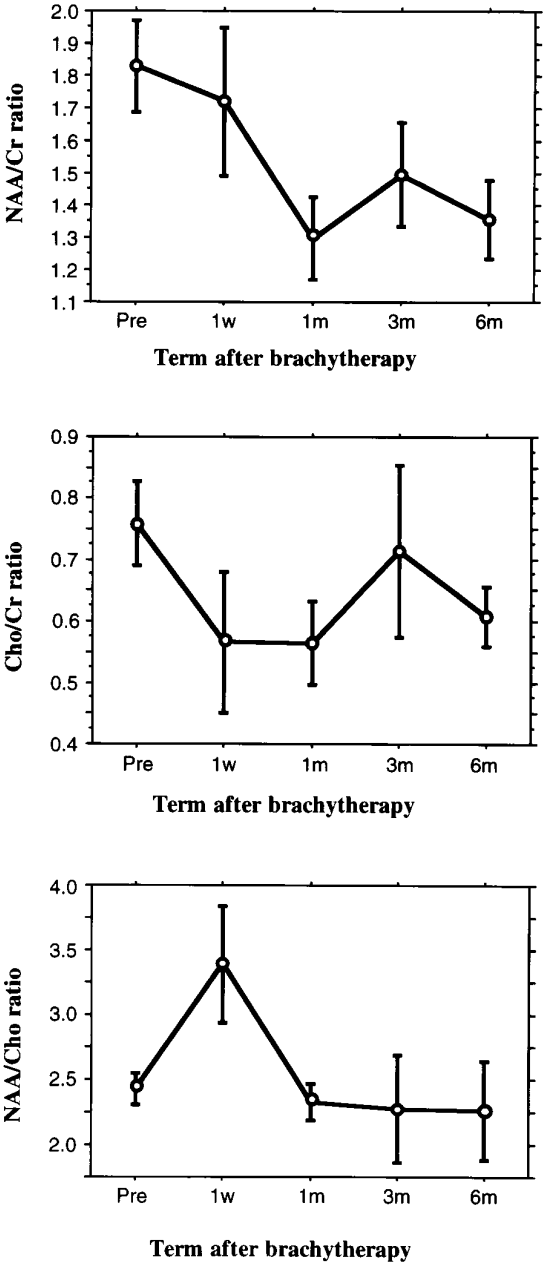


Fig 4. The time course of metabolic peaks at the contralateral (nonirradiated) hemisphere as shown by proton MR spectra in monkey brains. The ratios of NAA/Cr, Cho/Cr, and NAA/Cho 6 months after brachytherapy decreased as compared with those before treatment. These results suggest that brachytherapy has some effect on the contralateral (nonimplanted) hemisphere.

corresponding ratios for the irradiated contralateral hemisphere were 1.022 ± 0.400, 0.676 ± 0.242, and 1.500 ± 0.098, respectively. Compared with the ratios in patients with glioblastoma multiforme, there was a tendency for the ratios in patients with radiation necrosis to be close to 1.00. In particular, the ratio of NAA/Cho was significantly increased ($P < .005$).

These results demonstrate that, compared with glioblastoma multiforme, the proportion of metabolites in radiation necrosis have a tendency to approximate those of the irradiated contralateral (nonimplanted) hemisphere (Fig 7).

## Discussion

Phosphorus MR spectroscopy shows the energy status and pH in brain tissue (12–14). Proton MR spectroscopy provides information about energy and many other kinds of metabolism by tracking a large number of metabolites. In addition, proton MR spectroscopy has a better signal-to-noise ratio and spatial resolution than does phosphorus MR spectroscopy; therefore, it is practical for experimental and clinical studies to detect radiation-induced brain damage (15–17).

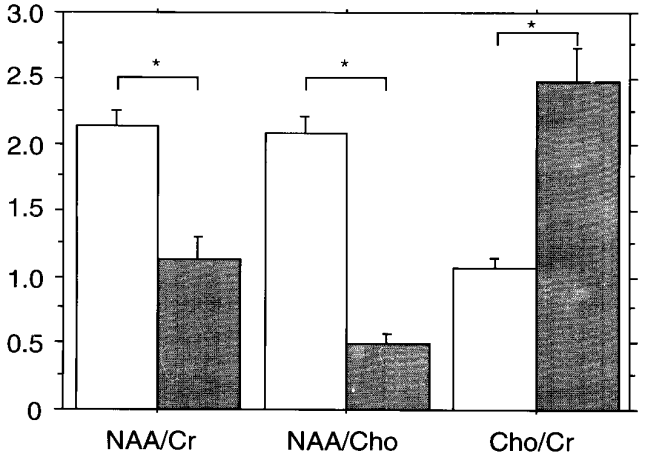


Fig 5. The ratios of metabolic peaks in patients with glioblastoma multiforme (n = 12) and in those without tumors (n = 16). The difference between these patients is significant ($P < .0001$). White indicates healthy volunteers; gray, patients with glioblastoma; and *asterisk*, $P < .0001$.)

Some experimental protocols have used MR spectroscopy to study the results of external radiation therapy on the brain. Grossmann et al (9) irradiated the brains of cats externally with a dose of 35 Gy and used phosphorus MR spectroscopy to observe the energy status and pH of the irradiated brain. In their study, the regions that showed changes on MR images were not significantly different from the phosphorus MR spectroscopic studies. Yousem et al (10) used proton MR spectroscopy to study the externally irradiated brains of cats who had been given a single dose of 50 Gy. They documented significant decreases in the NAA/Cr and NAA/Cho ratios in the irradiated hemisphere compared with the contralateral (nonirradiated) hemisphere, and found no differences or trends in the Cho/Cr ratios between hemispheres.

Interstitial brachytherapy has shown promising results in the treatment of some malignant brain tumors (18, 19). Focal enhanced lesions were seen after brachytherapy on contrast-enhanced T1-weighted MR images. Conventional imaging techniques (eg, CT or MR imaging) are unreliable in distinguishing radiation necrosis

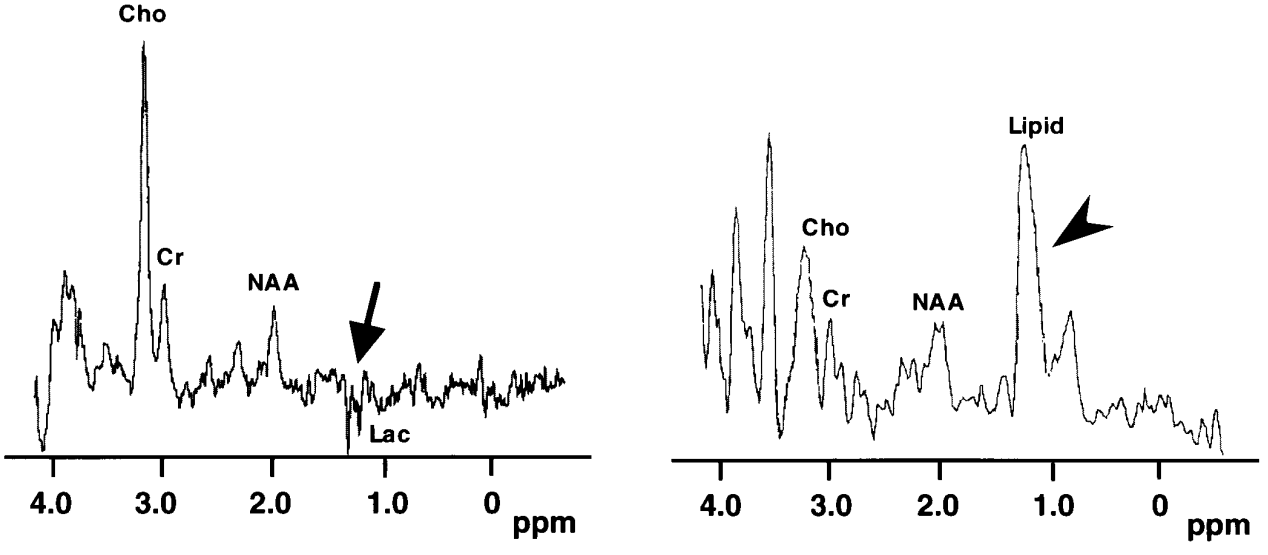


Fig 6. Typical proton MR spectra from glioblastoma multiforme (*left*) and radiation necrosis (*right*) in a patient. The peak height of Cho in radiation necrosis is relatively high compared with that in glioblastoma multiforme. The remarkable difference between glioblastoma multiforme and radiation necrosis is the existence of a lactate peak in glioblastoma multiforme (*arrow*) and the appearance of lipid peak in radiation necrosis (*arrowhead*).

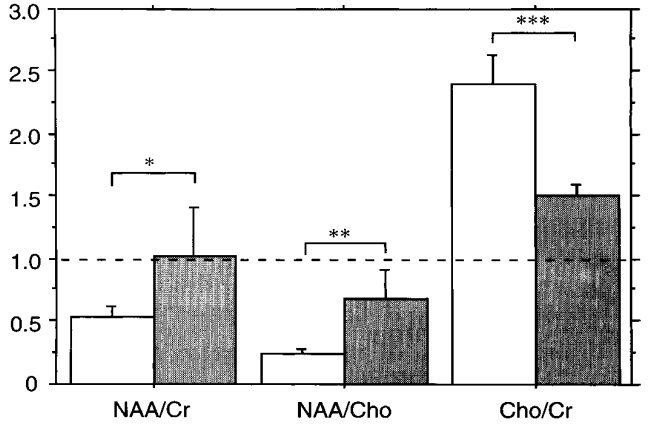


Fig 7. Metabolic ratios of treated hemispheres compared with those of contralateral hemispheres in patients with glioblastoma multiforme (n = 12; white) and radiation necrosis (n = 3; gray). The difference between the two groups is significant (*Asterisk* indicates $P = .074$; *double asterisk*, $P < .005$; and *triple asterisk*, $P = .094$). In comparison with patients with glioblastoma multiforme, the values of radiation necrosis are closer to 1.00.

from residual/recurrent gliomas in patients who are symptomatic after high-dose radiation therapy. Forsyth et al (20) have shown that stereotactic biopsy is useful in differentiating tumor progression from radiation necrosis, and Schwartz et al (21) have reported that dual-isotope single-photon emission CT (SPECT) with thallous chloride Tl 201 and $^{99m}$Tc hexamethylpropyleneamine oxime (HMPAO) was useful in differentiating sites of likely tumor growth from nonspecific radiation changes in patients treated for glioblastoma multiforme. Some authors have suggested that $^{201}$Tl SPECT could be used instead of positron emission tomography with fludeoxyglucose F 18 for patients with abnormal findings on CT or MR imaging who are referred for the detection of residual/recurrent brain tumor, especially when the lesion is 1.6 cm or more in diameter (22, 23). However, this opinion has been challenged (24–27).

In our animal study, metabolic peak ratios at the reference point showed remarkable changes 1 week after brachytherapy. Furthermore, the ratios of NAA/Cr and Cho/Cr at the reference point 6 months after brachytherapy had a tendency to decrease relative to those before treatment, because of destruction and decreased activity of neuronal cells in radiation-necrotic tissue (28, 29). Despite the remarkable differences in peak ratios at the reference point before and 6 months after brachytherapy, the metabolic peak ratios at the reference point 6 months after brachytherapy were not significant compared with those in the contralateral hemisphere after irradiation. Therefore, the concentration of all metabolites was low in the "pure" radiation necrosis that developed in normal brain tissue. Moreover, the proportion of metabolites in the established volume of interest centered on the reference point closely resembled that of the contralateral hemisphere after irradiation. In other words, these results show that the ratios between each of the metabolic peak ratios at the reference point and those of the contralateral hemisphere after treatment approached 1.00. We confirmed that brachytherapy had some effect on the contralateral (nonimplanted) hemisphere in our animal study.

In previous clinical proton MR spectroscopic studies, all spectra from malignant glioma had a lower NAA signal and a much higher Cho signal than normal brain. In addition, a lactate signal was sometimes observed (30–33). Our clinical studies confirmed these findings: in eight of 12 patients, the inverted doublet of lactate was shown at 1.3 ppm. On the other hand, the spectra from radiation necrosis in our patients had a low NAA signal and a high Cho signal, like that of patients with glioblastoma multiforme. In two of three patients, however, the lipid signal appeared as a broad-based peak at about 1.3 ppm. This peak was sharper than that of lipids seen in our animal study. It is possible that elevated lipid peaks reflect the presence of lipid-laden macrophages in necrotic tissue (34, 35).

Based on the metabolic peak ratios of untreated normal brain tissue, the peak ratios of both glioblastoma multiforme and radiation necrosis showed no significant differences, and the values of peak ratios were similar to those reported in previous studies (5, 16, 17, 30, 32, 33, 36, 37). These results imply that it may be difficult to differentiate radiation necrosis from malignant gliomas on the basis of comparisons of metabolic peak ratios with those in untreated healthy control subjects. However, our experimental findings showed that the irradiated peak ratios of the reference point nearly equaled those of the contralateral hemisphere. Metabolic peak ratios in all patients with radiation necrosis showed a pronounced tendency to be closer to those in the irradiated contralateral hemisphere than they did in patients with glioblastoma multiforme. In particular, the NAA/Cho ratio showed a significant difference ($P < .005$).

In our animal study, we confirmed that brachytherapy affected the contralateral hemisphere. Thus, the peak ratios of metabolites were not significantly different in radiation necrosis and in the irradiated contralateral hemisphere, despite the differences between radiation necrosis and untreated normal brain tissue. And in our clinical study, in which comparison was made with the contralateral hemisphere, radiation necrosis showed significant differences from glioblastoma multiforme. These patients had previously been treated by brachytherapy and whole-brain irradiation, and so it seemed that their contralateral hemisphere was also affected by irradiation. Therefore, we believe that the differences between radiation necrosis and glioblastoma multiforme in proton MR spectroscopic data were detected by comparing the metabolic peak ratios of lesions with those of the irradiated contralateral hemisphere. Our clinical data showed remarkable differences, especially in the NAA/Cho ratio. As for the cause of these results, it appears that the number of tumor cells decreased and that metabolism was depressed by irradiation in radiation necrosis and in the irradiated contralateral hemisphere. We postulate that radiation necrosis may be differentiated from glioblastoma multiforme by the proportion of NAA/Cho in relation to the irradiated contralateral hemisphere and by the appearance of the lipid signal.

In summary, our experimental and clinical studies analyzing the changes induced by brachytherapy with in vivo proton MR spectroscopy showed that metabolic peak ratios (NAA/Cr, NAA/Cho, and Cho/Cr) in radiation necrosis had characteristic features as compared with those of the irradiated contralateral hemisphere. In particular, the NAA/Cho ratio in radiation necrosis showed a significant difference from that of glioblastoma multiforme. We conclude that in vivo proton MR spectroscopy may be able to distinguish between necrosis and residual/recurrent glioblastoma multiforme.

## References


1. Bernstein M, Laperriere N, Leung P, et al. Interstitial brachytherapy for malignant brain tumors: preliminary results. *Neurosurgery* 1990;26:371–379
2. Chamberlain MC, Barba D, Kormanik P, et al. Concurrent cisplatin therapy and iodine 125 brachytherapy for recurrent malignant brain tumors. *Arch Neurol* 1995;52:162–167
3. Shrieve DC, Alexander E III, Wen PY, et al. Comparison of stereotactic radiosurgery and brachytherapy in the treatment of recurrent glioblastoma multiforme. *Neurosurgery* 1995;36:275–282
4. Aisen AM, Chenevert TL. MR spectroscopy: clinical perspective. *Radiology* 1989;173:593–599
5. Castillo M, Kwock L, Mukherji S. Clinical applications of proton MR spectroscopy. *AJNR Am J Neuroradiol* 1996;17:1–15
6. Hope PL, Moorcraft J. Magnetic resonance spectroscopy. *Clin Perinatol* 1991;18:535–548
7. Hubesch B, Marinier DS, Hetherington HP, et al. Clinical MRS studies of the brain. *Invest Radiol* 1989;24:1039–1042
8. Porter DA, Smith MA. Magnetic resonance spectroscopy in vivo. *J Biomed Eng* 1988;10:562–568
9. Grossman RI, Hecht-Leavitt CM, Evans SM, et al. Experimental radiation injury: combined MR imaging and spectroscopy. *Radiology* 1988;169:305–309
10. Yousem DM, Lenkinski RE, Evans S, et al. Proton MR spectroscopy of experimental radiation-induced white matter injury. *J Comput Assist Tomogr* 1992;16:543–548
11. Moonen CT, von-Kienlin M, van-Zijl PC, et al. Comparison of single-shot localization methods (STEAM and PRESS) for in vivo proton NMR spectroscopy. *NMR Biomed* 1989;2:201–208
12. Dempsey RJ, Combs DJ, Donaldson DL, et al. In vivo $^{31}$phosphorus spectroscopy during transient cerebral ischaemia in the gerbil. *Neurol Res* 1990;12:106–110
13. Hubesch B, Sappey-Marinier D, Roth K, et al. P-31 MR spectroscopy of normal human brain and brain tumors. *Radiology* 1990; 174:401–409
14. Petroff OA, Prichard JW, Behar KL, et al. Cerebral intracellular pH by $^{31}$P nuclear magnetic resonance spectroscopy. *Neurology* 1985;35:781–788
15. Heesters MA, Kamman RL, Mooyaart EL, et al. Localized proton spectroscopy of inoperable brain gliomas: response to radiation therapy. *J Neurooncol* 1993;17:27–35
16. Howe FA, Maxwell RJ, Saunders DE, et al. Proton spectroscopy in vivo. *Magn Reson Q* 1993;9:31–59
17. Posse S, Cuenod CA, Le-Bihan D. Human brain: proton diffusion MR spectroscopy. *Radiology* 1993;188:719–725
18. Matsumoto K, Tomita S, Sakurai M, et al. Interstitial brachytherapy for malignant gliomas using the Brown-Roberts-Wells (BRW) stereotactic system. *No Shinkei Geka* 1990;18:829–836
19. Matsumoto K, Nakagawa M, Higashi H, et al. Preliminary results of interstitial $^{192}$Ir brachytherapy for malignant gliomas. *Neurol Med Chir (Tokyo)* 1992;32:739–746
20. Forsyth PA, Kelly PJ, Cascino TL, et al. Radiation necrosis or glioma recurrence: is computer-assisted stereotactic biopsy useful? *J Neurosurg* 1995;82:436–444
21. Schwartz RB, Carvalho PA, Alexander E III, et al. Radiation necrosis vs high-grade recurrent glioma: differentiation by using dual-isotope SPECT with $^{201}$Tl and $^{99m}$Tc-HMPAO. *AJNR Am J Neuroradiol* 1991;12:1187–1192
22. Kahn D, Follett KA, Bushnell DL, et al. Diagnosis of recurrent brain tumor: value of $^{201}$Tl SPECT vs $^{18}$F-fluorodeoxyglucose PET. *AJR Am J Roentgenol* 1994;163:1459–1465
23. Moody EB, Hodes JE, Walsh JW, et al. Thallium-avid cerebral radiation necrosis. *Clin Nucl Med* 1994;19:611–613
24. Glantz MJ, Hoffman JM, Coleman RE, et al. Identification of early recurrence of primary central nervous system tumors by [18F]fluorodeoxyglucose positron emission tomography [see comments]. *Ann Neurol* 1991;29:347–355
25. Kim KT, Black KL, Marciano D, et al. Thallium-201 SPECT imaging of brain tumors: methods and results [see comments]. *J Nucl Med* 1990;31:965–969
26. Lilja A, Lundqvist H, Olsson Y, et al. Positron emission tomography and computed tomography in differential diagnosis between

recurrent or residual glioma and treatment-induced brain lesions. *Acta Radiol* 1989;30:121–128
27. Malkin MG. Interstitial irradiation of malignant gliomas. *Rev Neurol (Paris)* 1992;148:448–453
28. Miot E, Hoffschir D, Alapetite C, et al. Experimental MR study of cerebral radiation injury: quantitative T2 changes over time and histopathologic correlation. *AJNR Am J Neuroradiol* 1995;16: 79–85
29. Moseley ME, Cohen Y, Mintorovitch J, et al. Early detection of regional cerebral ischemia in cats: comparison of diffusion- and T2-weighted MRI and spectroscopy. *Magn Reson Med* 1990;14: 330–346
30. Barker PB, Glickson JD, Bryan RN. In vivo magnetic resonance spectroscopy of human brain tumors. *Top Magn Reson Imaging* 1993;5:32–45
31. Demaerel P, Johannik K, Van-Hecke P, et al. Localized $^{1}$H NMR spectroscopy in fifty cases of newly diagnosed intracranial tumors. *J Comput Assist Tomogr* 1991;15:67–76
32. Gill SS, Thomas DG, Van-Bruggen N, et al. Proton MR spectroscopy of intracranial tumours: in vivo and in vitro studies. *J Comput Assist Tomogr* 1990;14:497–504
33. Kugel H, Heindel W, Ernestus RI, et al. Human brain tumors: spectral patterns detected with localized H-1 MR spectroscopy. *Radiology* 1992;183:701–709
34. Chiang CS, McBride WH, Withers HR. Radiation-induced astrocytic and microglial responses in mouse brain. *Radiother Oncol* 1993;29:60–68
35. Di Chiro G, Oldfield E, Wright DC, et al. Cerebral necrosis after radiotherapy and/or intraarterial chemotherapy for brain tumors: PET and neuropathologic studies. *AJR Am J Roentgenol* 1988; 150:189–197
36. Miller BL. A review of chemical issues in $^{1}$H NMR spectroscopy: N-acetyl-L-aspartate, creatine and choline. *NMR Biomed* 1991;4: 47–52
37. Ott D, Hennig J, Ernst T. Human brain tumors: assessment with in vivo proton MR spectroscopy. *Radiology* 1993;186:745–752